Journal of Imaging Science and Technology® 53(1): 010503–010503-6, 2009.

Crystal Structure and Electrical Properties of a Quaternary Ammonium Salt Used as a Charge-Control Agent

K. Uta, Y. Sato, O. Yamate[†] and J. Mizuguchi[▲]
Graduate School of Engineering, Yokohama National University, 79-5 Tokiwadai, Hodogaya-ku, 240-8501 Yokohama, Japan
E-mail: mizu-j@ynu.ac.jp

Abstract. *The title compound (quaternary ammonium salt: P-51 from Orient Chemical Industries, Ltd.) is a well-known charge-control agent (CCA) used widely in electrophotography. Structure analysis and electrical measurements have been carried out in the present investigation in order to study its high thermal stability as well as to give more experimental evidence for our charge-control mechanism that assumes an appreciable temperature increase at the "toner/carrier" interface. P-51 is found to crystallize in a space group of $P2_1/n$. Observed unexpectedly were chains of OH⋯O intermolecular hydrogen bonds between the OH group of one anion and the O atom of the other, leading to a polymerlike stabilization of P-51, as characterized by a high melting point. On the other hand, the electrical conductivity is shown to increase exponentially with temperature by 2 to 3 orders of magnitude in the temperature range between room temperature and 100°C. This supports out our charge-control mechanism. © 2009 Society for Imaging Science and Technology.*
[DOI: 10.2352/J.ImagingSci.Technol.(2009)53:1(010503)]

INTRODUCTION

Charge-control agents (CCAs) are widely used in electrophotography to create a desired charge level and polarity. Aside from the CCA performance, a high thermal stability is also required for CCAs because pulverized toners are usually prepared by kneading various toner components such as polymer, colorant, CCA, etc. at about 130–180°C. The title compound (P-51 from Orient Chemical Industries, Ltd.: Figure 1) is a commercial CCA of the positive type. Previously, Sukata and others investigated P-51 and its derivatives from the standpoint of crystallinity and kinetics of the tribocharging.[1,2] These authors stressed particularly the importance of the crystalline state for the tribocharging characteristics rather than the amorphous one.

A number of investigations have been carried out on the charge-control mechanism on the basis of the effective electric field,[3,4] work function,[5] mass transfer,[6] and charge transfer.[7] However, no clear-cut, consistent explanation has been established at the moment. In view of the present situation, we have recently proposed a novel model that assumes an appreciable temperature increase at the "toner/carrier" interface due to the triboelectrification.[8] Because of the present local and instantaneous heating, the electrical conductivity of the CCA (which resides on the surface of both toner and carrier) is remarkably increased to give a conductive channel through which the carrier-flow occurs effectively to charge up the toner. These two assumptions have been experimentally verified.[8] Especially, the local heating up to around 100°C has been confirmed by using a pigment marker (ethylpyridylperyleneimide) that changes its color from black (*trans* form) to red (*cis* form). Around this temperature, the electrical conductivity of CCA increases remarkably by 2 to 3 orders of magnitude as compared with that of room temperature.

The purpose of the present investigation is to first, clarify the high thermal stability of P-51 from the crystal structure, because ordinary quaternary ammonium salts (used often as supporting electrolytes in electrochemistry) possess only low melting points under 100°C. Second, we intend to elucidate the correlation between the crystal structure, the temperature dependence of the electrical conductivity, and the charging characteristic of the toner.

EXPERIMENT

Materials and Crystal Growth of P-51

P-51 (melting point: ca. 190°C) is a commercial product of Orient Chemical Industries, Ltd. Single crystals were grown by recrystallization from a methanol solution. After 48 h, a number of colorless, transparent crystals were obtained in the form of blocks (size: $0.49 \times 0.26 \times 0.17$ mm^3).

Data Collection and X-ray Structure Analysis

Reflection data were collected on a R-Axis Rapid-F diffractometer from Rigaku using Cu$K\alpha$ radiation ($\lambda = 1.5418$ Å)

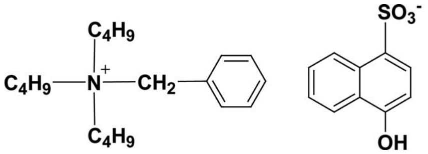

Figure 1. Molecular structure of P-51.

[†] Present address: Orient Chemical Industries, LTD., 541-0057 Osaka, Japan.

[▲] IS&T Member.

Received May 5, 2008; accepted for publication Oct. 27, 2008; published online Feb. 4, 2009.
1062-3701/2009/53(1)/010503/6/$20.00.

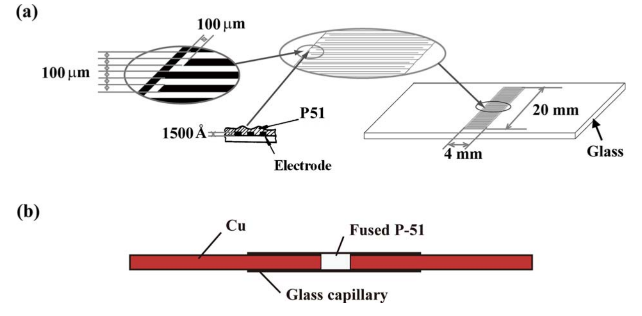

Figure 2. Experimental setup: (a) recrystallized sample and (b) fused sample.

at room temperature and −180°C. The structure was solved by direct methods (SIR2004[9]) and refinement was carried out by the full-matrix least-squares method on F^2 (SHELXL-97[10]).

Preparation of Recrystallized and Fused Samples

Measurements of the electrical conductivity in the form of powders are often not very reproducible and reliable due to the packing density of the powder as well as the electroding problems. Therefore, two kinds of samples were prepared: (a) recrystallized sample and (b) fused sample. The former was prepared by spin coating a methanol solution directly on a glass substrate with ITO (indium-tin-oxide) interdigital electrodes [Figure 2(a)]. The latter was prepared in a glass capillary (diameter: 2.3 mm) with Cu-rod electrodes by heating the powder above the melting point, followed by a gradual cooling to room temperature so as to obtain an entirely transparent sample [Fig. 2(b)].

Measurements

The temperature dependence of the electrical conductivity was measured with a 6514 Keithley electrometer in the temperature range between room temperature and 200°C at a heating rate of 3 K/min. Thermogravimetric analysis (TGA) and differential thermal analysis (DTA) were made under N_2 on commercial powders, recrystallized powders, and fused powders of P-51 at a heating rate of 10 K/min, using a Rigaku Thermo Plus TG-8120. Powdered x-ray diffraction diagrams were measured at room temperature with a RAPID-F on commercial, recrystallized, and fused powders of P-51s. Simultaneous measurements of both diffraction diagram and DSC (differential scanning calorimetry) was also carried out on commercial powders under N_2 with a Rigaku Ultima III XRD/DSC equipment in the temperature range between 20 and 200°C. The heating rate was 2 K/min. Triboelectrification measurements were made on toners composed of styrene acryl resin (100 parts), carbon black (6 parts), wax (2 parts), and CCA (1 part) in accordance with the standard procedure specified by ISJ, using a blow-off equipment (TB-200: Toshiba Chemical).

RESULTS AND DISCUSSION

Crystallographic Parameters for P-51

Table I details the crystallographic parameters for P-51 measured at room temperature.[11] Figure 3(a) shows the ORTEP plot of P-51. The molecule has no center of symmetry (i.e., C_1), but a pair of the molecules reside on an inversion center. Since one negative charge is delocalized in the form of SO_3^-, no significant difference in S–O bond length is recognized between these three bonds. To our great surprise, there are chains of OH···O intermolecular hydrogen bonds in anions between the OH group of one anion and the O atom of another as shown in Fig. 3(b). Figure 4 illustrates the molecular arrangement of P-51, composed of an anion polymer backbone and quaternary ammonium cations. The present structure is quite similar to that of an ion-exchange resin. The present hydrogen bonds impart a polymerlike stabilization to P-51, resulting in the increase of the melting temperature.

Table I. Crystallographic parameters for P-51.

Formula	$C_{29}H_{41}NO_4S$
Molecular weight	499.71
Crystal system	Monoclinic
Space group	$P2_1/n$
a (Å)	14.3810(11)
b (Å)	9.8124(7)
c (Å)	19.7757(15)
β (°)	92.560(5)
Z	4
Density (g/cm^3)	1.190
R	0.049

Powder X-ray Diffraction Diagrams

Figure 5 shows the powder x-ray diffraction diagrams for three different powders of P-51: commercial, recrystallized, and fused samples. The diagram of the commercial powder coincides perfectly with that of the recrystallized one. In addition, this phase is identified as the same as the single crystal. On the other hand, fused P-51 exhibits an entirely different diffraction diagram as characterized by amorphouslike poor crystallinity. This diagram is basically in good agreement with that of Sukata et al. as obtained by quenching a molten P-51.[1]

Temperature Dependence of the XRD/DSC Diagrams of Commercial P-51

Figure 6(a) shows the XRD diagrams for commercial P-51 measured in the temperature range between 20 and 200°C. The diffraction diagrams remain unchanged up to around 160°C. Then, a significant change in diffraction diagrams (2θ=7, 12–13, 21, and 24°) was observed 160 and 175°C, indicating a phase change. After that, the sample melted at about 190°C. Fig. 6(b) is the detailed XRD/DSC diagrams for the process before and after the phase change at 167°C. An endothermic peak around 167°C in the DSC curve bears out the phase change. The second phase exists, however, only in a narrow temperature range between 167°C and the melting point of 186°C. It is also remarkable to note that the

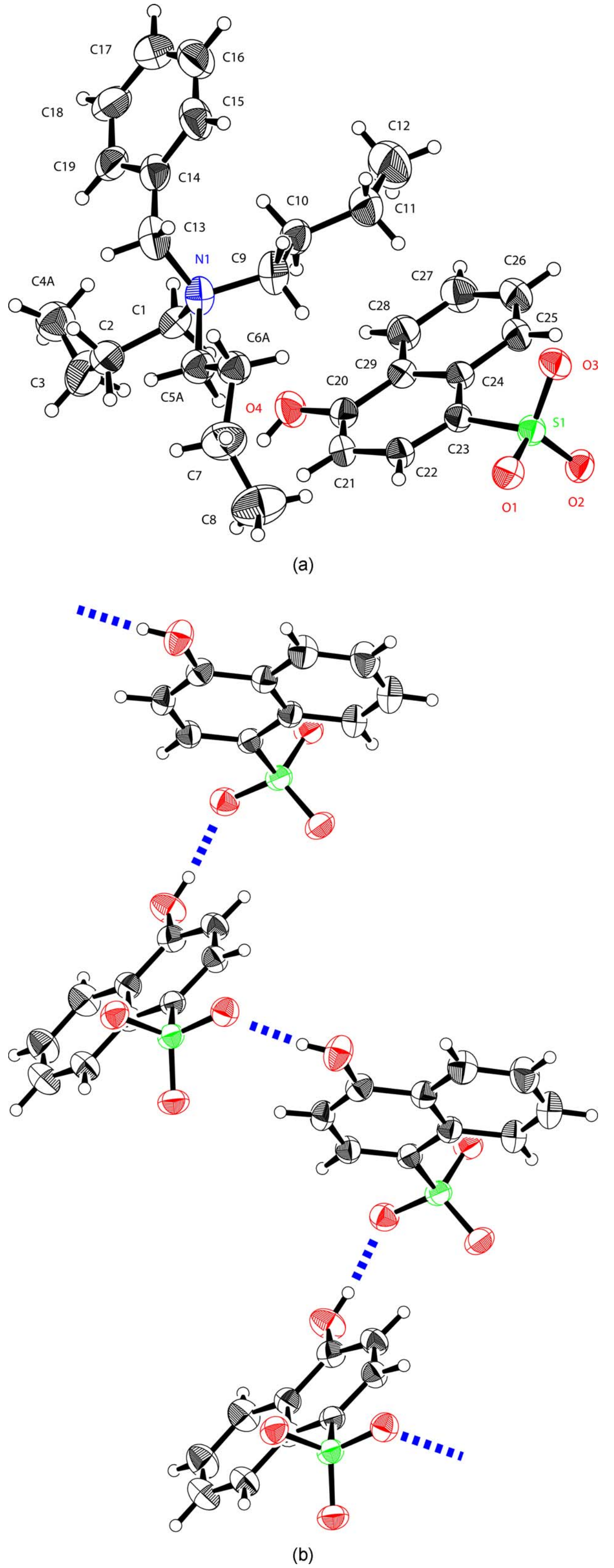

(a)

(b)

Figure 3. (a) ORTEP plot of P-51 and (b) formation of OH⋯O intermolecular hydrogen bonds in anions. Hydrogen-bond geometry (O4-H4⋯O1): O4-H4 = 0.82 Å, H4⋯O 1 = 1.83 Å, O4⋯O 1 = 2.657(2) Å, and the angle of O4/H4/O1 = 169°.

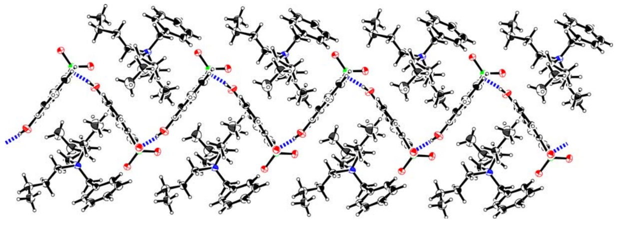

Figure 4. Molecular arrangement of P-51, showing an anion polymer-backbone together with quaternary cations.

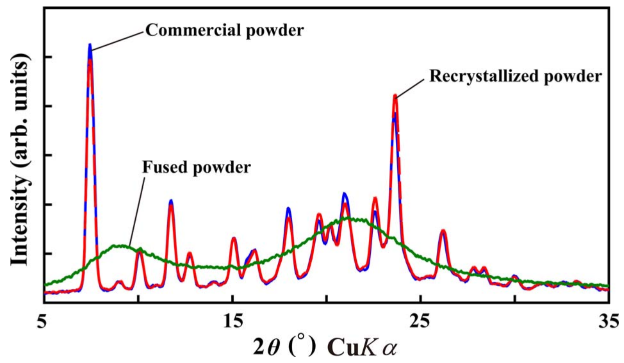

Figure 5. Powder x-ray diffraction diagrams for commercial, recrystallized, and fused powders of P-51s. Measurements were made by a Rigaku Rapid-F.

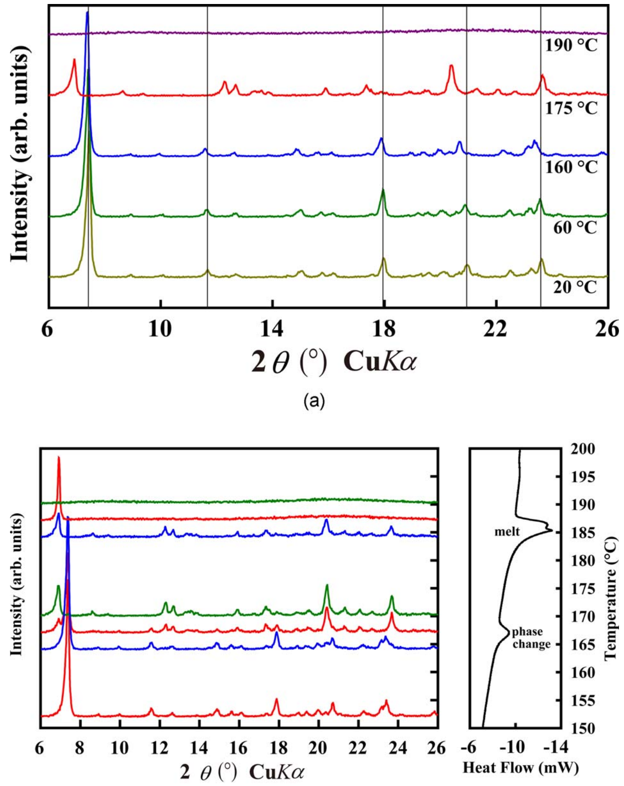

(a)

(b)

Figure 6. (a) XRD diagrams for commercial P-51 measured in the temperature range between 20 and 200 °C and (b) detailed process before and after the phase change at 167 °C. Measurements were made by a Rigaku Ultima III.

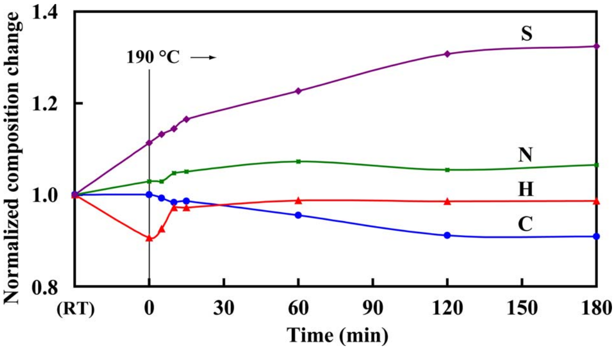

Figure 7. Composition change of P-51 in the fused state of 190°C as a function of time on the basis of the elementary analysis. The C, H, N, and S values were normalized by those of RT.

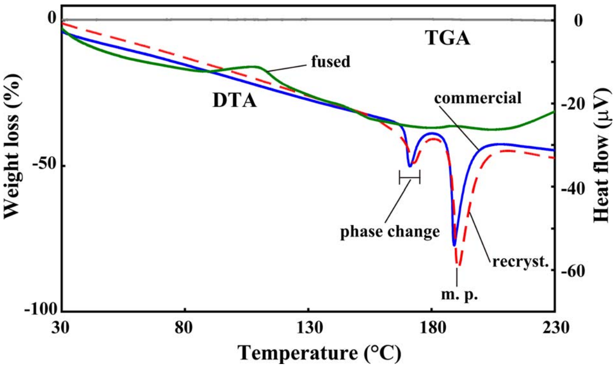

Figure 8. TGA/DTA curves for commercial, recrystallized, and fused powders of P-51.

sample gave off an offensive smell near the melting point around 175°C, indicating partial decomposition of P-51.

The above odor emission is closely related to the composition change of P-51 in the fused state of 190°C, as shown in Figure 7, where the C, H, N, and S components were normalized to those at room temperature (RT). In the heating process from room temperature to 190°C in air, the S and H components started to increase and decrease, respectively, while the N and C components remained almost unchanged. Then, the temperature was kept constant at 190°C. Further composition change was observed with elapse of time, especially in the S, C, and N components. This indicates that the composition change becomes more significant as the retained time in the fused state is longer. In fact, the sample cooled down immediately after fusion is still powderlike (or can be pulverized) at room temperature, but very brittle. On the other hand, the sample retained for a couple of minutes in the fused state looks like a polymer and cannot be pulverized anymore. In addition, the polymer-like fused sample exhibits neither phase change nor melting point in TGA/DTA measurement, as described below. The above observations suggest that P-51 is no longer reversible once it is heated above 175°C.

TGA/DTA Curves

Figure 8 shows the TGA/DTA curves for three different samples of P-51: commercial, recrystallized, and fused powders. Among these, fused P-51 (prepared by immediate cooling after fusion) appeared somewhat brittle. No weight loss is observed in all samples in the range between 30 and 230°C; whereas the DTA curves are drastically different. Commercial and recrystallized P-51s behave nearly in the same way and exhibit a gradual, endothermic curve, which ends up with two peaks at about 170 and 190°C. The endothermic peak around 170°C corresponds to the phase change shown in Fig. 7; whereas the peak at about 190°C corresponds to the melting point of P-51. However, there is a slight difference between the commercial and recrystallized powders. On the other hand, fused P-51 behaves entirely different in the DTA curve. That is, fused P-51 exhibits neither endothermic peak around 170°C (i.e., no phase change) nor melting point around 190°C. This indicates that the heating above the melting point results in a different compound characterized by an amorphouslike phase (Fig. 5).

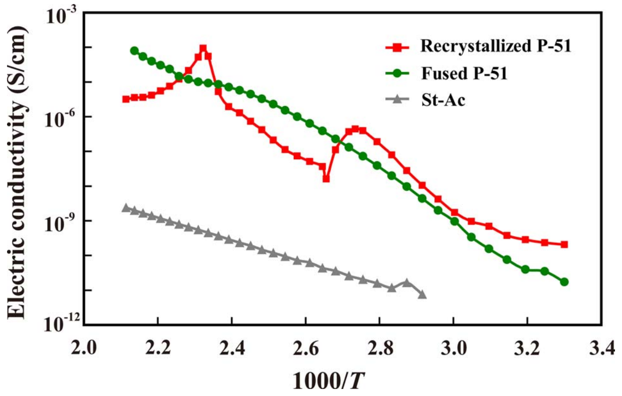

Figure 9. Temperature dependence of the electrical conductivity: recrystallized P-51, fused P-51, and St-Ac polymer.

Temperature Dependence of the Electrical Conductivity

Figure 9 shows the temperature dependence of the electrical conductivity (i.e., Arrhenius plot) for recrystallized and fused P-51s together with a fused styrene-acryl (St-Ac) polymer used widely as a binder in toners. The electrical conductivity increases linearly with temperature in these samples, showing semiconductorlike behavior. It is remarkable to note that recrystallized P-51 exhibits two bumps, peaking at about 90 and 160°C; whereas fused P-51 is characterized by a swell in the temperature range up to 160°C. The conductivity bump at about 160°C corresponds to the phase change as verified by the XRD/DSC experiments [Fig. 6(b)] and also by the DTA curve (Fig. 8). As seen from Fig. 9, the electrical conductivity at 100°C is higher than that of room temperature by 2 to 3 orders. On the other hand, the electrical conductivity of St-Ac polymer is always lower than that of P-51s by 2 to 3 orders of magnitude. This indicates that P-51 serves as a conductive channel between toner and carrier, while the electrical charge is expected to reside on St-Ac polymer. This supports our proposed charge-control mechanism described in the Introduction.[8]

As for the conductivity bump at about 90°C, no explanation is available at the moment.

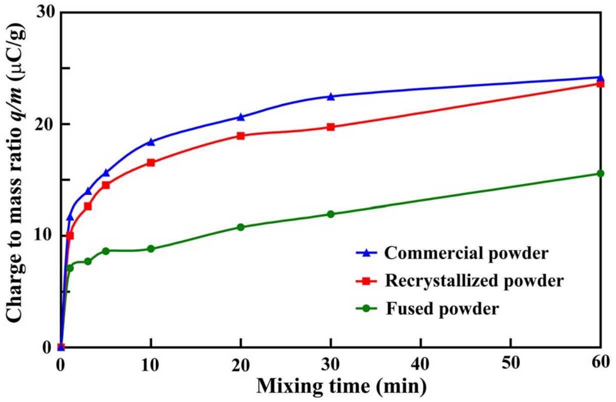

Figure 10. Charging characteristics for toners with various P-51s: commercial, recrystallized, and fused samples.

Triboelectrification of Toners which Include P-51

Figure 10 shows the charging characteristics as a function of time. Commercial and recrystallized P-51s exhibit excellent charging characteristics, whereas the amount of charge of fused P-51 is much lower, no difference in charging rate is recognized in these three samples.

Figures 11(a)–11(c) are the scanning electron microscope (SEM) pictures for commercial, recrystallized, and fused P-51s, respectively. These samples were sieved in advance with a mesh of 5 μm. A number of crystallites characterized by beautiful habits are observed in commercial and recrystallized P-51s. On the other hand, fused P-51 lacks this property and appears brittle. This is presumably due to an amorphous-like state. The brittle particles are considered to possess poor adhesion to the toner or carrier surface. Because of this, the brittle particle is probably not in the position to provide a conductive channel in the triboelectrification process, through which the carrier flow occurs to charge the toner. This could be a tentative explanation why fused P-51 shows an inferior charging characteristic to the recrystallized one.

CONCLUSIONS

The conclusions drawn from the present investigation can be summarized as follows.

1. P-51 is found to crystallize in space group of $P2_1/n$. There are chains of OH···O intermolecular hydrogen bonds in anions. The present hydrogen-bond network is responsible for the high thermal stability of P-51 characterized by a high melting point of 190°C.

2. The phase of commercial P-51 coincides with that of recrystallized P-51. On the other hand, fused P-51 is characteristic of an amorphouslike phase and no longer exhibits a melting point.

3. P-51 undergoes a phase change around 167°C. The new phase exists, however, only in a narrow temperature range between 167°C and the melting point of 186°C. In addition, the present phase is thermally not so stable, because some volatile components vaporize above 175°C, accompanied by an offensive odor.

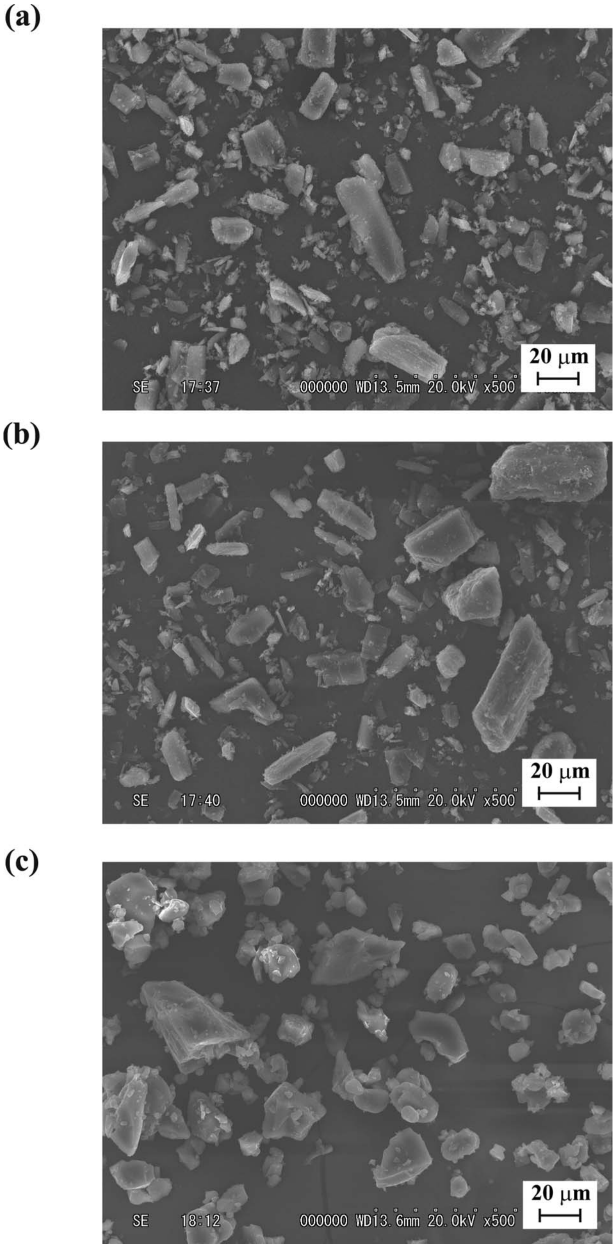

Figure 11. SEM pictures: (a) commercial P-51, (b) recrystallized P-51, and fused P-51.

4. The temperature dependence of the electrical conductivity of recrystallized or fused P-51 shows an increase in electrical conductivity by 2–3 orders of magnitude with increasing temperature. However, recrystallized P-51 shows two bumps in electrical conductivity (90 and 160°C). The latter is caused by the phase change while the former remains unclarified.

5. Commercial and recrystallized P-51s are confirmed to exhibit excellent charge-control characteristics. On the other hand, the charging characteristic is inferior in fused P-51. This is presumably due to the brittle, amorphous-like state of fused P-51, which leads to a low adhesion force to the toner or carrier surface.

REFERENCES

[1] K. Sukata, S. Itoh, C. Matsushima, and T. Kihara, “Mechanism of the action of charge control agents (CCA) I: Importance of the crystal and its surface conditions in quaternary ammonium type CCA”, J. Imag. Soc. Jpn. **34**, 167–172 (1995) (in Japanese).

[2] K. Sukata, S. Itoh, S. Yamanaka, and S. Sugawara, “Mechanism of the action of charge control agents (CCA) II: Kinetic model and kinetics of the tribocharging of model toners using quaternary ammonium-type CCA,” J. Imag. Soc. Jpn. **34**, 167–172 (1995) (in Japanese).

[3] L. B. Schein, “Theory of toner charging”, J. Imaging Sci. Technol. **37**, 1–4 (1993).

[4] L. B. Schein, “Electric field theory of toner charging”, J. Imaging Sci. Technol. **44**, 475–483 (2001).

[5] R. J. Nash, M. L. Grande, and R. N. Muller, “CCA effects on the triboelectric charging properties of a two-component xerographic developer”, *Proc. IS&T’s NIP 17* (IS&T, Springfield, VA, 2001) pp. 358–364.

[6] A. Suka, M. Takeuchi, K. Suganami, and T. Oguchi, “Toner charge generated by CCA particles at the interface between toner and carrier”, J. Imag. Soc. Jpn. **45**, 127–132 (2006).

[7] J. Guay, J. E. Ayala, and A. F. Diaz, “The question of solid-state electron transfer in contact charging between metal and organic materials”, Chem. Mater. **3**, 1068–1073 (1991).

[8] J. Mizuguchi, A. Hitachi, Y. Sato, and K. Uta, “Study of the charge control mechanism of charge control agents”, J. Imaging Sci. Technol. **52**, 030506 (2008).

[9] M. C. Burla, R. Caliandro, M. Camalli, B. Carrozzini, G. L. Cascarano, L. De Caro, C. Giacovazzo, G. Polidori, and P. Spagna, “SIR2004: An improved tool for crystal structure determination and refinement”, J. Appl. Crystallogr. **38**, 381–388 (2005).

[10] G. M. Sheldrick, “A short history of SHELX”, Acta Crystallogr., Sect. A: Found. Crystallogr. **A64**, 112–122 (2008).

[11] J. Mizuguchi, Y. Sato, K. Uta, and K. Sato, “Benzyltributylammonium 4-hydroxynaphthalene-1-sulfonate”, Acta Crystallogr., Sect. E: Struct. Rep. Online **E63**, o2509-o2510 (2007).